Paleostress analysis and petrography of Newer Dolerite Dykes from Ghatagaon and surrounding area of North Odisha Singhbhum Craton

A Thesis

submitted in partial fulfillment of the requirements for the MSc

Degree Programme

by

Paritosh Bhattacharyya

20226402

Indian Institute of Science Education and Research

Pune 411008, India

April, 2024

Under the guidance of

Dr. Durga Prasanna Mohanty

Geology Department

Savitribai Phule Pune University

This thesis is dedicated to my parents and my late maternal grandmother

भारतीय विज्ञान शिक्षा एवं अनुसंधान संस्थान पुणे
INDIAN INSTITUTE OF SCIENCE EDUCATION AND RESEARCH PUNE
An Autonomous Institution of the Ministry of Education, Govt. of India

CERTIFICATE

This is to certify that the thesis entitled **"Paleostress analysis and petrography of Newer Dolerite Dykes from Ghatagaon and surrounding area of North Odisha Singhbhum Craton"**, towards the fulfillment of the degree of Master of Science in Geology programme at the Indian Institute of Science Education and Research, Pune, represents study/work carried out by **Mr. Paritosh Bhattacharyya (20226402)** at Savitribai Phule Pune University, under the supervision of **Dr. Durga Prasanna Mohanty,** Assistant Professor, Department of Geology, Savitribai Phule Pune University, during the academic year 2023-2024.

Dr. Durga Prasanna Mohanty
Assistant Professor
Department of Geology
Savitribai Phule Pune University, 411007

Declaration

I hereby declare that the research work presented in the report entitled **Paleostress analysis and petrography of Newer Dolerite Dykes from Ghatagaon and surrounding area of North Odisha Singhbhum Craton** have been carried out by me at the Department of Geology, Savitribai Phule Pune University, Pune under the supervision of **Dr. Durga Prasanna Mohanty** and the same has not been submitted elsewhere for any degree.

Paritosh Bhattacharyya

Paritosh Bhattacharyya

MSc 2nd year

20226402

Dr. Durga Prasanna Mohanty
Assistant Professor
Department of Geology
Savitribai Phule Pune University, 411007

Acknowledgments

I would like to express my deepest gratitude to Dr. Durga Prasanna Mohanty for his invaluable guidance, unwavering support, and insightful feedback throughout the entire duration of my MSc thesis. His expertise, patience, and guardianship have been instrumental in shaping this research and in my personal and academic growth.

I am also immensely thankful to Dr. Sudipta Sarkar for graciously sharing his expertise and for serving as the expert advisor for my thesis. His invaluable insights and constructive criticism have greatly enriched the quality of this work.

I would also like to extend my cordial thanks to my family, friends, and colleagues for their encouragement, understanding, and unwavering belief in me throughout this journey.

I am also indebted to Mr. Bishuddhakshya Puhan for his constant support and guidance. The expertise and patience he put into the fieldwork is the reason I could able to complete my thesis within time.

Lastly, I acknowledge the contributions of my fellow colleague Gopinath Nayak along with all the individuals who generously shared their time, knowledge, and experiences, without whom this thesis would not have been possible.

Contents

List of figures

Abstract

Singhbhum Craton is a major geological province situated in the eastern part of India, which has significant mineral deposits. The area has experienced a number of tectonic events, and the analysis of paleostress using dykes can shed light on its deformation history. The objective of this thesis is to carry out a paleostress analysis of the Singhbhum Craton using structural data from the orientation of dykes in parts of North Odisha Singhbhum Craton. In structural geology, measuring stress is crucial for comprehending how rocks behave and deform within the Earth's crust. It gives important information about tectonic movements, geological history, and the mechanical characteristics of rocks. The methodology for this study involves fieldwork and structural analysis. The fieldwork involves measuring the orientation of dykes in the study area and mapping them. The paleostress can be found by a) stress from faults b) from fault slip inversion (brittle deformation) or c) using magmatic pressure and tectonic stress correlation. Here we have specifically discussed about the third method in greater detail in this regard. The primary purpose of this study is to identify the extent of paleostress that has impacted the North Odisha Craton of Singhbhum and its history of deformation. The secondary objective is to provide information on tectonic processes that had affected mineral deposition in the area and detailed classification of the dykes using petrography. The paleostress analysis of the Singhbhum Craton is a crucial study that will contribute to our understanding of its regional geological history. The results of this study will be beneficial for mineral exploration and resource management in the area. This thesis proposal outlines the methodology and expected results of the study. It is anticipated that the study would offer insightful information about the deformation history of North Odisha Singhbhum Craton.

1. Introduction

A Craton is an old and stable part of continental lithosphere that consists of crust and uppermost mantle. Cratons are usually located in the interior side of a tectonic plate. Ancient basement crystalline rock essentially makes up the cratons which may be covered by younger sedimentary rocks. The term craton is used to differentiate the part of continental lithosphere that is different from the part that is tectonically active over longer geological period. Such a craton is Singhbhum Craton that is believed to be built by successive granitic magmatism primarily in three major phases at ~3.52 Ga, ~3.47-3.43Ga, and ~3.40-3.35 Ga. These magmatic events resulted in Tonalite-Trondhjemite-Granodiorite (TTG)-type suites and some more younger events occurred at 3.32-3.35 Ga, and 3.31-3.28 Ga giving rise to granitic-granodioritic magma (Mukhopadhyay and Matin, 2019). In geological terrains, the mafic dyke swarms emplacement plays a great role as significant time indicator. The shield terrains have been intruded by the Precambrian dyke swarms over wider geological time period. Therefore, these dykes contribute to our understanding of Proterozoic tectonics, magmatism and continental reconstruction. Similarly, the Indian Shield protocontinents, such as the Singhbhum, Bastar, Dharwar, and Aravalli-Bundelkhand protocontinents, had encountered dyke swarm incursions with varying features and orientations. The Precambrian Singhbhum granitoid complex in the Singhbhum craton was invaded by an extraordinary group of dyke swarms known as the “Newer dolerite dyke swarm” across a broad geological time period spanning from 2800 to 1100 Ma. Albeit there are already established studies that focus on petrogenesis and geochemistry of the dykes of Singhbhum Cratonic province (e.g. R. Mir, 2022; Dasgupta, P. et al., 2019; Manu Prasanth MP, Pang K-N, Hari KR, Sahoo BB, Ravindran A and Iizuka Y, 2023; Ray, Arijit., 2012; Shankar. Ravi. et al., 2014 amongst others), still there are not much studies available that deal with the paleostress or the fluid pressure (P_f) conditions using the dyke orientations. In order to do this, it is necessary to use dyke orientations to plot the 3D Mohr stress circle and estimate the relative stress/P_f conditions. The findings must then be connected to regional deformation. This is a tried-and-true method that has also been used to determine the stress level in veins and dykes with different compositions, such as aplite, quartz, and pegmatite dykes (e.g., Jolly and Sanderson, 1995; Jolly and Sanderson, 1997; Mondal and Mamtani, 2013; Mazzarini et al., 2011).

Fractures of the upper crust of the earth provide plane for the fluid to come out. Dykes are instances of similar kind of fluid outpour and they have been noticed to encroach along pre-existing fractures (Currie and Ferguson, 1970; Baer et al., 1994). The method of constructing a three-dimensional Mohr circle was developed by Jolly and Sanderson (1997) to study the stress and fluid pressure conditions that resulted in the opening of pre-existing fractures during the emplacement of dykes. It was based on the methods employed by Delaney et al. in 1986, which states that magma can fill in older joints if the magma pressure is greater than the horizontal stress across the joint plane. The pre-existing fractures can only open when P_f surpasses the normal stress (σ_n) (Delaney et al., 1986). Therefore to establish the three dimensional Mohr Circle the orientations of the intruded dykes are crucial in calculating the stress associated with regional scale deformation and Specifically, this is the topic of our current work.

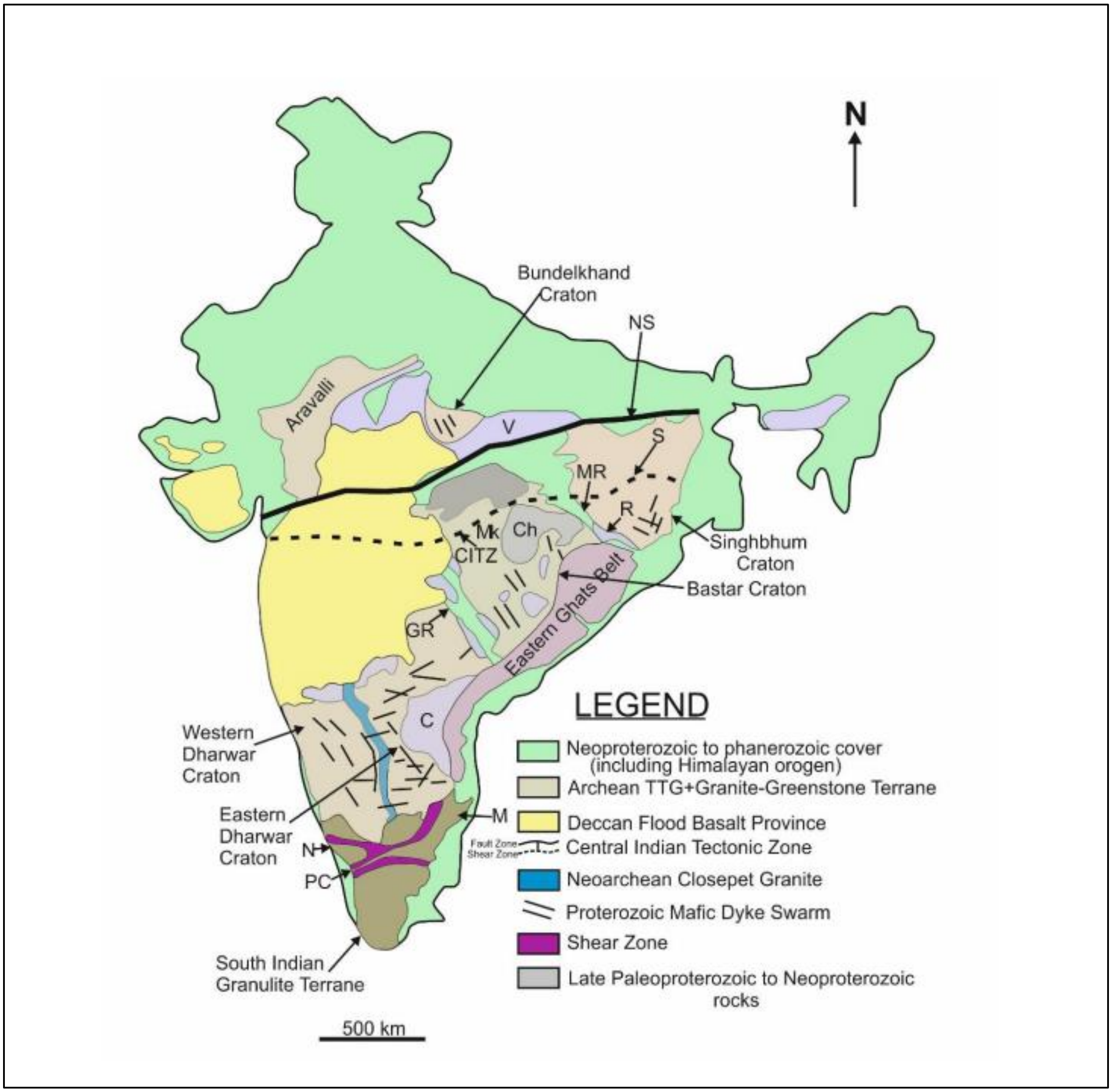

Figure 1 Map depicting the broader geology and tectonics of the Indian subcontinent, including Precambrian mafic dyke swarms that intersect with Archean cratons. (Singhbhum Craton along with other Indian cratonic blocks) (modified after French et al., 2008).

2. General Geology of the study area:

2.1. Geological framework of the Singhbhum Craton:

2.1.1. Configuration and characteristics:

One of Peninsular India's oldest cratonic blocks, the Singhbhum Craton makes upto an area of around 39,000 km2 and forms a North-South elongated oval shaped block in eastern India, ranging from 21°N to 22.75°N and 84.5°E to 86.5°E.

The Singhbhum Craton, which spans about 40,000 km2 across Odisha, Jharkhand and surrounding territories in the east side of the Indian Shield, is encompassed by two mobile belts that of Proterozoic in age: the Eastern Ghat Mobile Belt to the south of it and the Satpura Mobile Belt to the east, north, and north-west side. The Bastar and Singhbhum cratons are divided from each other by the Mahanadi Graben. The craton is mostly made up of granitoid rocks, ranging in age from 3.5 - 2.5 billion years (Mukhopadhyay, 2001). The Singhbhum Craton, which is repository to some of the oldest rocks found on the Indian subcontinent, is distinguished by a profusion of banded iron formation (BIF) that is closely linked to basic volcanics and ultrabasic intrusives, as well as by tonalitic and granodioritic gneisses and granites. The craton is thought to have formed as an outcome of periodical compressive deformations what has been named the Singhbhum Orogeny by Saha, 1994.

2.1.2. The tectonic limits of Singhbhum Craton:

The curvilinear Singhbhum Shear Zone (SSZ) demarcates the outline of the Singhbhum Craton against Chota Nagpur Gneissic Complex in the north. This is also known as “Copper Belt Thrust”. It is a 1-5 kilometers vast terrain of fractures. A portion of the fractures made it to the mantle, opening doors to erupting lava flows and places where plutons, that are ultrabasic in nature may be found (Banerji, 1962, 1969, 1977). The Sukinda Thrust outlines the southern tectonic limit of the Singhbhum. There are several parallel faults connected to the Sukinda Thrust. Among these is the 100-kilometer-long

Sarapalli–Gundlichanal Fault, which marks the edge of the chromite bearing ultrabasic horizon. The Iron Ore Group (IOG) is separated from Gondwana Basin by the Sukinda Thrust. The Sukinda Thrust further further goes into south-west in the Eastern Ghat region as The Terrane Boundary Shear Zone . (Biswal and Sinha, 2003).

The SSZ is crossed by the Eastern Indian Tectonic Zone (EITZ), which delineates the boundaries to the east of the Singhbhum Craton. It extends northward along the Craton's eastern boundary.

2.2. Lithostratigraphy of Singhbhum Craton:

The lithostratigraphic layout of Singhbhum Cratonic Province can be divided into six major lithotectonic units (Fig). They in geochronological order are as follows: Older Metamorphic Group (Champua Group), the Saraikela Gneiss (Older Metamorphic Tonalite Gneiss), the Singhbhum Granite Type A, the Iron Ore Group, the Singhbhum Granite Type B and the Darjin Group (Sarkar and Saha, 1962,1988; Mukhopadhyay, 2001). Moreover there are also Malangtoli Volcanics, the Newer Dolerite dyke swarms, and the Jagannathpur Volcanics suite in addition. The late Proterozoic Singhbhum orogeny caused many deformations in these lithostratigraphic units.

Champua Group is the oldest group in the Singhbhum Craton. Singhbhum Granite Type B makes up the major portion. The OMG and OMTG have minor occurrences within the terrain. The Singhbhum Granite Type A serves as the foundation for the Iron Ore Group and its accompanying supracrustals. Singhbhum Granite Type B, a later phase granite, intrudes into Iron Ore Group. Third granitic activity caused this younger granite that made up the central and the eastern part of the batholithic complex.

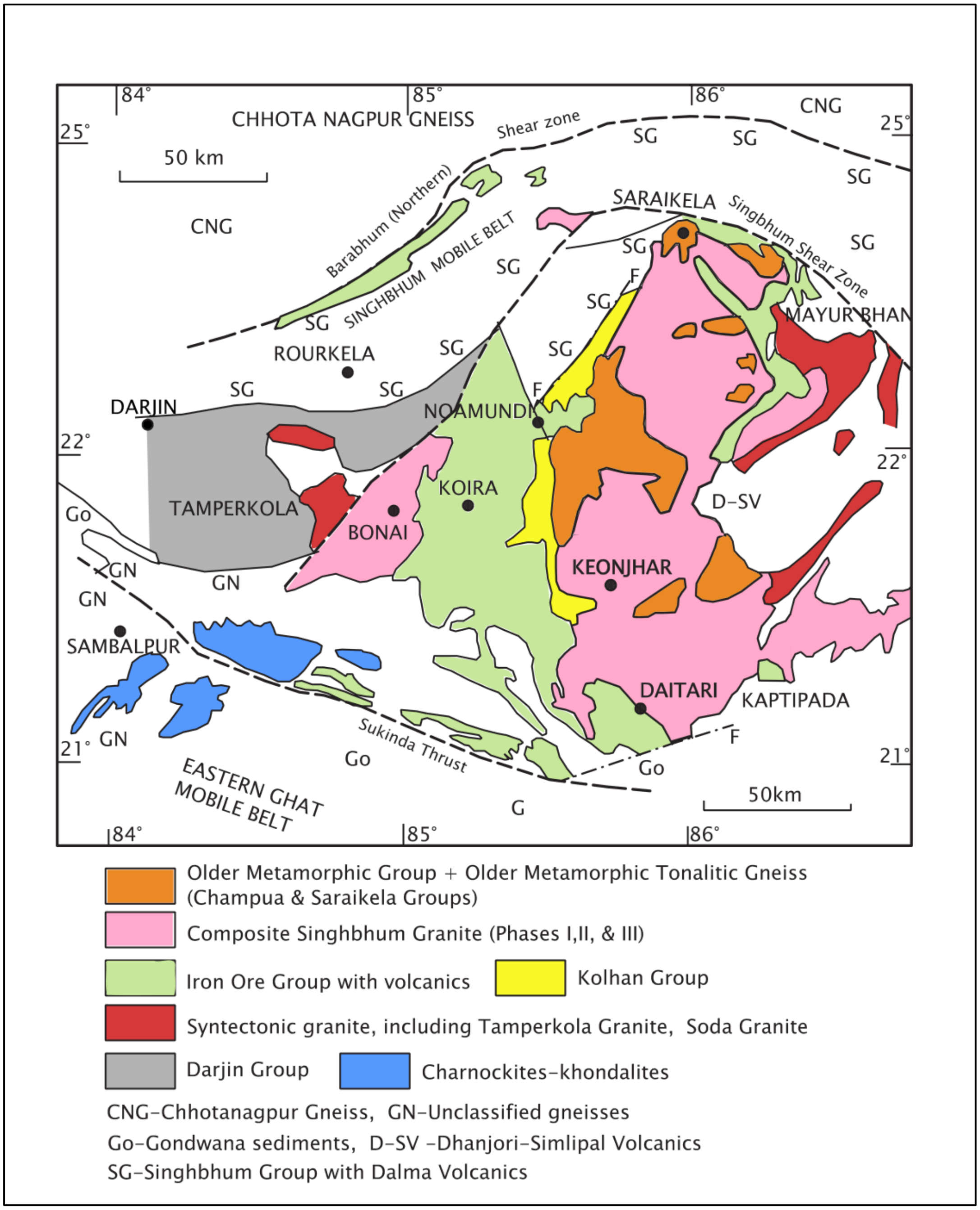

Figure 2 Generalized map of Singhbhum craton focusing mainly on the Archaean lithotectonic units (Modified after Sarkar 2000; Saha et al. 2004).

2.2.1. Champua Group

This is the oldest lithostratigraphic unit of the Singhbhum Craton. The Older Metamorphic Group is found in small outcrops spanning in size from a few square kilometers to several hundred square kilometers. This group mainly forms enclaves. Champua, located southwest of Gorumahisani, is characterized by pelites, sandstones, and ferromagnesian lithologies. This is where the alternative name Champua Group comes from. The Champua rocks underwent amphibolite-facies metamorphism, resulting in the formation of different types of schists and amphibolites approximately at 600 to 650 °C temperature and 5 to 5.5 kbar pressure (Saha et al., 1984). The orthoamphibolite of Champua succession is a tholeiite-affinity magma with a slightly enriched LREE and flat HREE pattern. That indicates partial melting from mantle and low Nd isotope count (Sharma et al.,1994). The Sm–Nd isochron age of the orthoamphibolite shows 3305 ± 60 Ma—the age of magma crystallization.

2.2.2. Saraikela Gneiss

Tonalite intrusion altered the older sequence, resulting in the formation of a complex with amalgam of Champua metamorphics and the intruding tonalites. This is called the "Older Metamorphic Tonalite Gneiss" (Saha, 1994). The OMTG rocks are located in an area of approximately 900 km^2 east and south of Champua, as well as lesser outcrops near Seraikela, Onlajori, Bahalda, Rairangpur, and Thakurmunda. Prabhakar and Bhattacharya (2013) restrict the term OMTG only to the enclaves of migmatitic tonalite gneisses within the Singhbhum Granite (SBG). The name Saraikela Gneiss came from a outcrop with similar association that was found in the north of Saraikela area in Jharkhand that too belongs to Older Metamorphic Tonalite Gneiss. Trace-elements study of Saraikela Gneiss suggests that the partial melting of amphibolites of OMG gave rise to the tonalite magma. This is a characterizing feature of Saraikela Gneiss (Mukhopadhyay 2001). The Saraikela Gneiss is thought to be roughly 3400 Ma old. It underwent extensive metamorphism approximately 3200 million years ago.

2.2.3. Singhbhum Granite Type A (Besoi Granite)

The primary three major pulses of granitic magmatism made up the whole batholithic complex. Among them the first two phases (Phases I and II) of intrusion produced the Singhbhum Granite Type A also known as the Besoi Granite. (Saha et al., 1984, Saha, 1994). This Granite spanned over a larger are in the Keonjhar district and has been well dated in the Besoi area of Mayurbhanj district. That is where the alternative name ‘Besoi Granite’ came from. Phase I is composed of potassium-poor granodiorite-trondhjemite, while the later phases are monzogranite and granite (Saha, 1994). The Pb-Pb age of this Granite shows around 3442 ± 26 Ma (Ghosh et al., 1996).

2.2.4. Iron Ore Group

The Iron Ore Group, consisting of slightly metamorphosed ferruginous sediments and basic volcanics, unconformably lies above the Besoi Granite (Murty and Acharya, 1975; Mukhopadhyay, 1976; Banerji, 1977; Iyengar and Murthy, 1982). There are three main volcano-sedimentary belts where the Iron Ore Group occurs. They are as follows: the western Iron Ore Group belt (Noamundi Jamda Koira belt), the Iron Ore Group belt of east (Gorumahishani-Badampahar belt) and the southern Iron Ore Group belt (Tomka-Daitari belt).

2.2.5. Singhbhum Granite Type B (Bonai Granite)

Singhbhum Granite Type B makes up majority of the granite batholith. This is the outcome of third phase (Phase III) of granitic magma emplacement and it intrudes the older Iron Ore Group at several places (Saha 1994). The porphyritic trondhjemite that makes up the Bonai pluton, which spans 500 km2 and is located at the western side of the main batholithic complex, has a chemistry that is identical to the earlier two phases. The Pb-Pb age of Bonai Granite shows around 3163 ± 26 Ma (Sengupta et al., 1991).

2.2.6. Darjin Group and Tamperkola Granite

In the western side of the Singhbhum Batholithic complex, the Drajin Group lies unconformably over the Iron Ore Group and the Bonai Granite. This group is little metamorphosed and undeformed and is made up of cross-bedded and conglomeratic sandstones, subarkosic sandstones, shales and dolomitic limestones (Mahalik, 1994). A pink coloured Tamperkola Granite intrudes the Darjin Group.

3. Fieldwork: observations and field photo representation

3.1. Location of the study area:

Dyke swarms from North Odisha Singhbhum Craton were primary concern while carrying out the fieldwork. There are numerous dykes those have intruded the granitic province of North Odisha. The fieldwork was mainly carried out in and around Keonjhar district, Odisha. The places include Anandapur, Ghasipura, Ghatagaon, Dhenkikote & Bhimkund. Roadside sections are accessible by NH20 that runs through Anandapur to Keonjhar.

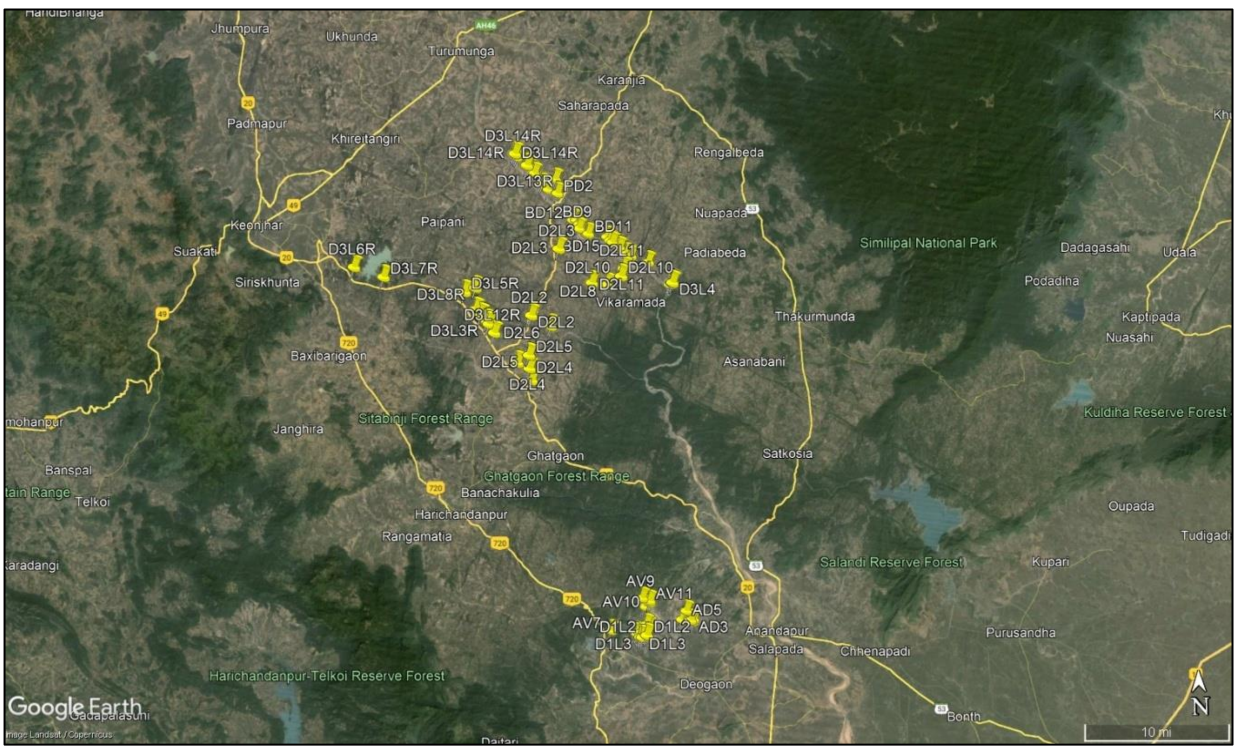

Figure 3 Satellite view of the field area showing locations from where dyke orientations have been taken

3.2. Field Observations:

Several dyke swarms have affected the North Odisha Singhbhum cratonic province. The most general trend of the dykes is NW-SE and NE-SW, with some places exhibiting crosscut relationship. In Geology the general thumb rule is that the feature which seems to be crosscut another feature is exclusively younger in age. The grain size of the dyke rocks varies substantially from place to place indicating different cooling processes and crystallizing timings under different circumstances. The intruding dykes also exhibit varying thickness ranging from a meter to several meters (fig 4 and 5). Depending upon the width of the pre-existing fractures the dyke thickness changes significantly. In many places the dyke orientations (steep dip) support the dykes to be intruding near vertically. As per the literature study suggests, the Singhbhum granites are belong to three distinct phases. In later stage, at Neoproterozic time, the dykes are intruded into the granitic terrain. At some places the dykes show exceptionally well sharp contact with the granitic host rock (Fig 4b,c,d,e,f)). Around 149 dyke orientations have been taken in the field to carry out with further proceedings (Table 1).

3.3. Representative Field Photographs:

Figure 4


g
W
E
h
Host
Dyke
N
S
Contact
i
Contact
S
N
dyke
Host
j
NE
Contact
Dyke
Host
K
W
E
Dyke
Host rock
(Granite)

Figure 5

Fig 4 (a) Dyke in map view. A dyke intruding the granitic country rock is clearly seen in Google Earth Pro. (b) The same NW-SE trending dyke of Bhimkund region in outcrop view. The dyke intrudes the granitic host leaving a well developed sharp contact. (c) Contact between the granitic host rock and the dyke is clearly visible. Cooling joints developed at the direction perpendicular to the trend of the dyke. (d) A sharp contact between the host and the dyke is distinctly seen. Cooling joints are also seen to be developed perpendicular to the dyke trend. (e) Contact is clearly visible. Cooling joints are also found perpendicular to the dyke trend. The width or thickness of this particular dyke can be easily determined from this section. The thickness of the intruding dyke is about 2.5 meters. (f) Baitarani River section. Another NE-SW trending dyke is found to be intruding the granitic country rock leaving a clear contact between two.

Fig 5 (g) A dyke is found to be intruding through the ground. A contact is barely seen. (h) A sharp contact is visible between the dyke and the granitic country rock. (i) A contact is seen between the dyke and the country rock. The country rock granite has been lateritized extensively. The contact is also not very sharp. (j) The granitic host has been turned into laterite and a NE-SW trending dyke has been intruded the country. The dip of the contact plane is not uniform; rather it changes from bottom to top. (k) A dyke has been almost vertically intruded the country rock on the bank of Baitarani River.

4. Methodology:

4.1. Condition for opening a fracture:

The upper crust of the earth is permeated by numerous fractures which act as planes allowing the fluid to come out. Dykes are examples of such fluid flow and have been observed intruding along pres-existing fractures (Currie and Ferguson, 1970; Roberts and Sanderson, 1971; Baer et al., 1994; Jolly and Sanderson, 1995).

For the fluid to open a pre-existing fracture, the fluid pressure (P_f) must surpass the normal stress (σ_n) acting on the fracture walls (Delaney et al., 1986).

$$P_f \geq \sigma_n \tag{1}$$

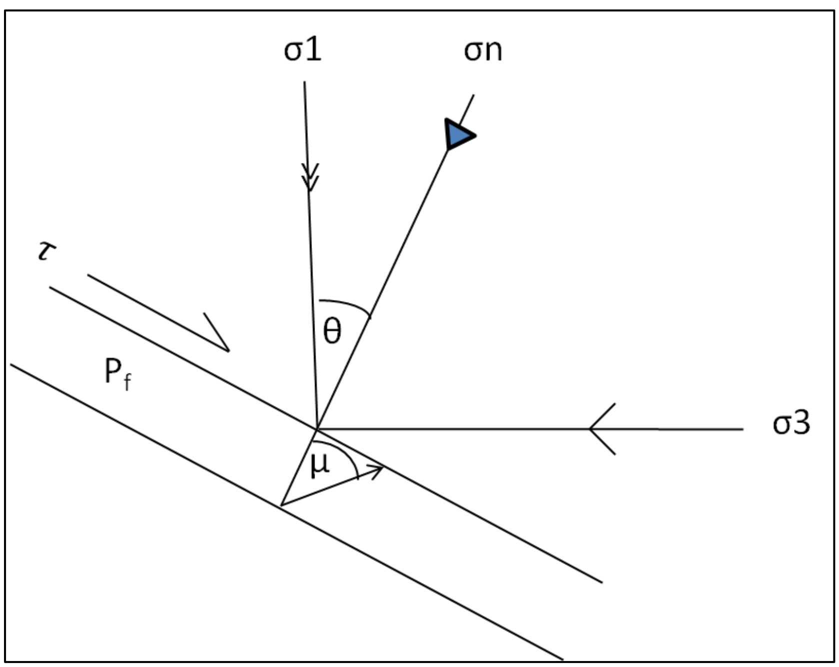

Figure 6 The notations used in analysis of a fracture dilated by fluid. σ_1 , σ_3, σ_n are maximum principal stress, minimum principal stress and the normal stress acting on that surface respectively. The angle between the maximum principal stress and the normal to the surface is denoted as θ. τ is the shear stress acting on the surface. μ denotes the direction of fracture opening.

4.2. Mohr Circle:

4.2.1. Introduction

Mohr Circle is a graphical manifestation used in material science, engineering and structural geology to analyze stress states. Named after the German engineer Otto Mohr, this circle visually represents stress components and their relationship, aiding in the determination of principal stresses, maximum shear stresses and stress transformations. By providing a geometric representation of stress conditions, Mohr Circle simplifies complex stress analysis and facilitates a better understanding of material behaviour under various loading conditions. Mohr Circle is plotted on a diagram with normal stress as the abscissa (X-axis) and shear stress as the ordinate (Y-axis). The diameter of the Mohr circle and/or its position changes with the variation in deformation conditions (temperature, confining pressure, fluid pressure and strain rate). This can result in rupture and thus provide vital information about the behaviour of the material under the specific deformation condition.

Mohr circle helps us to calculate normal and shear stresses and the orientation of a plane in rocks. The main points to be noted are:

1. For a given state of stress, the shear and normal stresses acting on a specific plane (through a point), are represented on the Mohr circle.
2. The orientation as well as magnitude of the normal stress and shear stress during brittle failure is depicted by Mohr circle.
3. It does not take into account the geographical reference frame, but shows the sense of motion (dextral or sinistral) along a plane.
4. It predicts the relationship between rock strength and state of stress under which the rock fractures.

It is crucial to understand that the orientation and size of the area on which the force is acting, in addition to the force's magnitude and orientation, affect the amount of stress. A few presumptions must be made in order to find the Mohr circle's equation:

1. There is no rotation or translation, and the entire system is in an equilibrium state with no relative movement.
2. Tension is interpreted as negative, while the body's compression is depicted as positive.
3. Principal stresses represent the state of stress.

4.2.2. Stress acting on a plane:

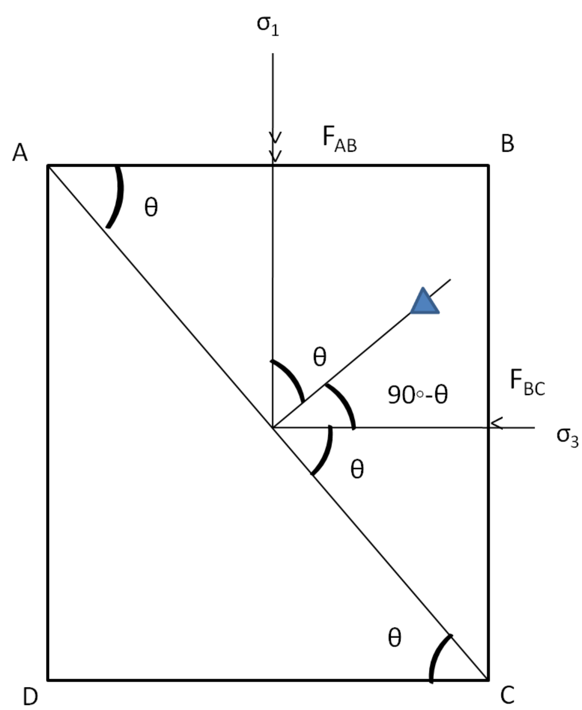

Figure 7 Force (F) acts on a surface area (A)

From fig 7,

From ΔABC,

Area of AB plane, $A_{AB} = AC \cos\theta$ (2)

Area of BC plane, $A_{BC} = AC \sin\theta$ (3)

Stress σ = Force/Unit area = F/A

$\sigma_1 = F_{AB}/A_{AB}$

or, $F_{AB} = \sigma_1 * A_{AB}$

or, $F_{AB} = \sigma_1 * A_{AC} \cos\theta$ (From 2) (4)

Similarly, $F_{BC} = \sigma_3 * A_{AC} \sin\theta$ (From 3) (5)

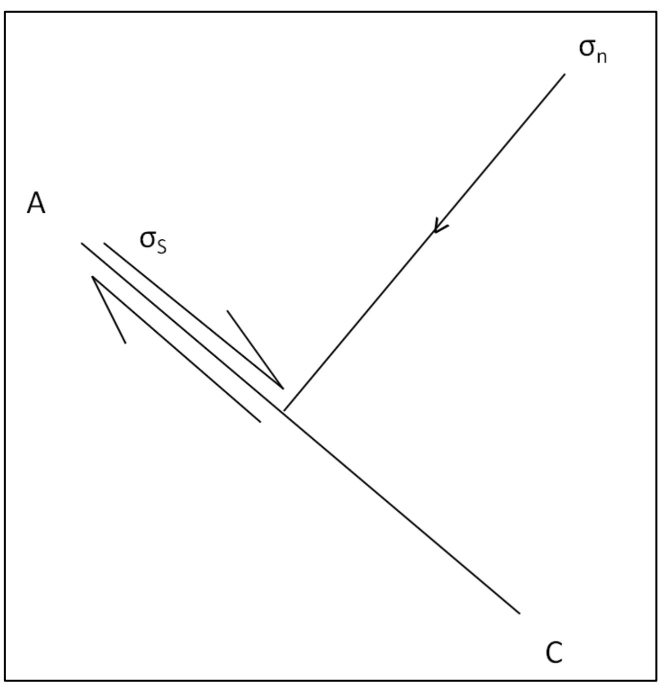

Figure 8 The total force is resolved into normal stress (σ_n) and shear stress (σ_S)

From fig 8,

$\sigma_n = F_{Perpendicular}/A_{AC}$

or, $\sigma_n * A_{AC} = F_{Perpendicular}$

or, $\sigma_n * A_{AC} = F_{AB} \cos\theta + F_{BC} \sin\theta$

or, $\sigma_n * A_{AC} = \sigma_1 * A_{AC} \cos^2\theta + \sigma_3 * A_{AC} \sin^2\theta$ (From 4 & 5)

or, $\sigma_n = \sigma_1 \cos^2\theta + \sigma_3 \sin^2\theta$

or, $\sigma_n = \sigma_1 \cos^2\theta + \sigma_3 - \sigma_3 \cos^2\theta$

or, $\sigma_n = \sigma_3 + \cos^2\theta (\sigma_1 - \sigma_3)$

or, $\sigma_n = \sigma_3 + 1 + \cos 2\theta/2 * (\sigma_1 - \sigma_3)$

or, $\sigma_n = \frac{\sigma_1+\sigma_3}{2} + \frac{\sigma_1-\sigma_3}{2} \cos 2\theta$ (6)

Similarly,

$\sigma_s = F_{Parallel} */ A_{AC}$

or, $F_{Parallel} = \sigma_s * A_{AC}$

or, $\sigma_s * A_{AC} = F_{AB} \sin\theta - F_{BC} \cos\theta$

or, $\sigma_s * A_{AC} = \sigma_1 A_{AC} \sin\theta \cos\theta - \sigma_3 A_{AC} \sin\theta \cos\theta$

or, $\sigma_s = \sin\theta \cos\theta (\sigma_1 - \sigma_3)$

or, $\sigma_s = \frac{\sin 2\theta}{2} (\sigma_1 - \sigma_3)$ (7)

The general equation of a circle is $(x-h)^2 + (y-k)^2 = r^2$ (8)

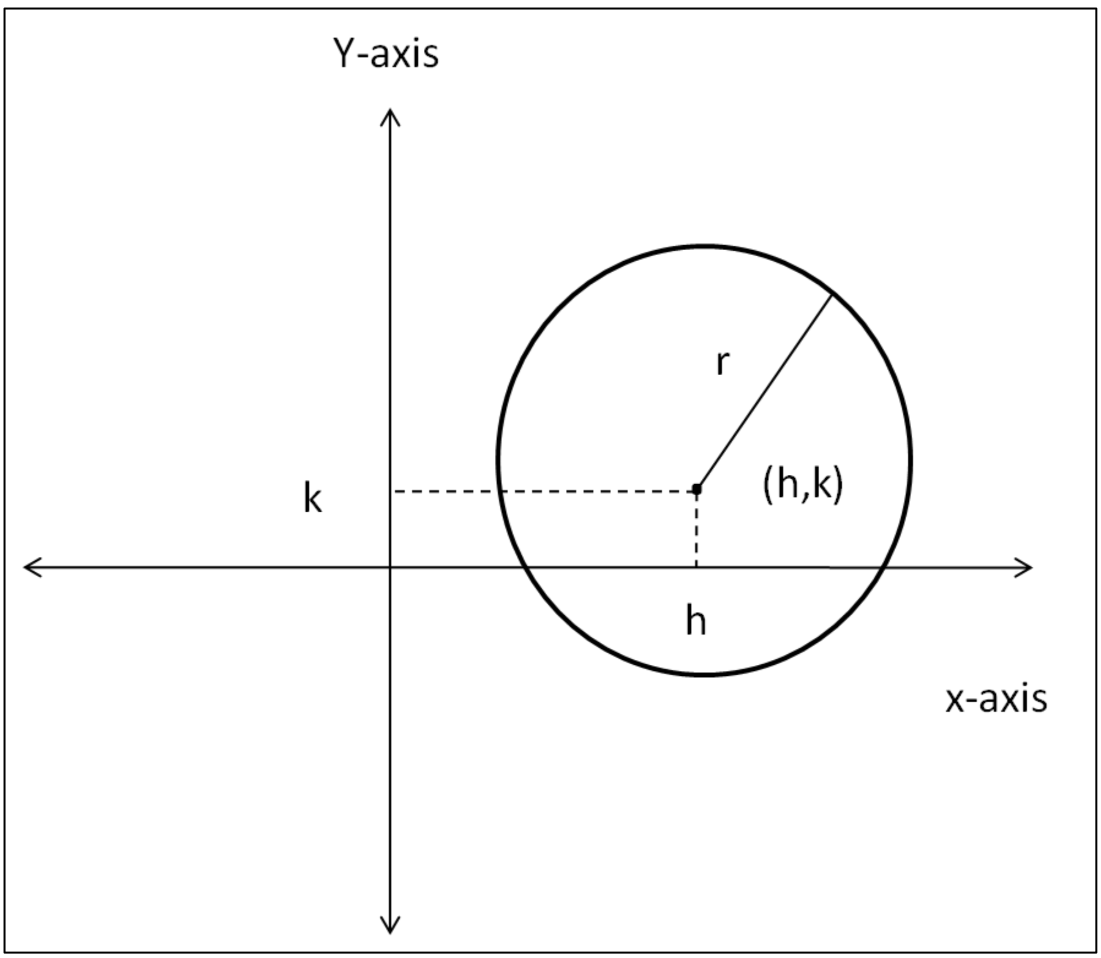

Figure 9 A circle, (h,k) of which marks the centre of it and r denotes the length of its radius.

Continuing with eq. 6,

$\sigma_n = (\sigma_1 + \sigma_3)/2 + (\sigma_1 - \sigma_3)/2 \cos 2\theta$

or, $\{\sigma_n - (\sigma_1 + \sigma_3)/2\}^2 = \{(\sigma_1 - \sigma_3)/2\}^2 \cos^2 2\theta$ (9)

Similarly from eq. 7,

$\sigma_s = \sin 2\theta/2\ (\sigma_1 - \sigma_3)$

or, $\sigma_s^2 = \{(\sigma_1 - \sigma_3)/2\}^2 \sin^2 2\theta$ (10)

Adding eq. 9 & eq. 10,

$\{\sigma_n - (\sigma_1 + \sigma_3)/2\}^2 + \sigma_s^2 = \{(\sigma_1 - \sigma_3)/2\}^2 \cos^2 2\theta + \{(\sigma_1 - \sigma_3)/2\}^2 \sin^2 2\theta$

or, $\{\sigma_n - (\sigma_1 + \sigma_3)/2\}^2 + (\sigma_s - 0)^2 = \{(\sigma_1 - \sigma_3)/2\}^2$,[as $\sin^2 2\theta + \cos^2 2\theta = 1$] (11)

Comparing it with the general equation of circle (equation 8),

$g \equiv \frac{\sigma_1+\sigma_3}{2}$

$h \equiv 0$

$r \equiv \frac{\sigma_1-\sigma_3}{2}$

The mean stress and deviatoric stress components of the stress matrix are represented in two dimensions by the centre and radius of the Mohr circle respectively. The normal stress and shear stress exhibit variation based on the plane's orientation (θ).

4.2.3. Comparison of Mohr space and real space in 2D:

Let's assume that maximum principal stress (σ_1) is acting on a plane AB. CD is the normal to that plane. The angle between the maximum principal stress and the normal to the plane is θ (Fig 10)

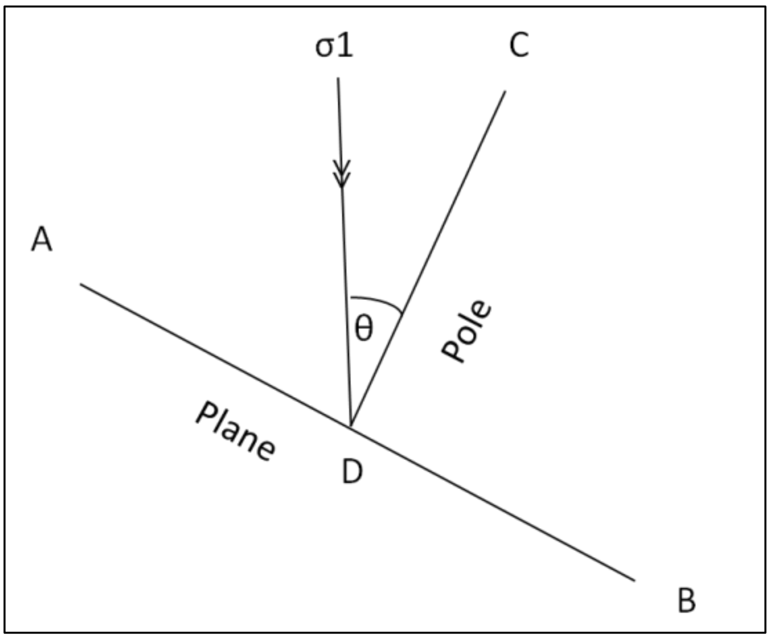

Figure 10 In real space σ1 is acting on a plane and the angle between σ1 and normal to the plane is θ.

The plane AB can be presented graphically through the Mohr circle ('P1' point in Fig 11).

In the Mohr space σ1 and σ3 are plotted on the horizontal axis (Fig.11). Therefore the angle between them is 180°. But in real space σ1 and σ3 are perpendicular. Hence in Mohr space the angle will be twice of Real space and thus θ will be 2θ in Mohr Space.

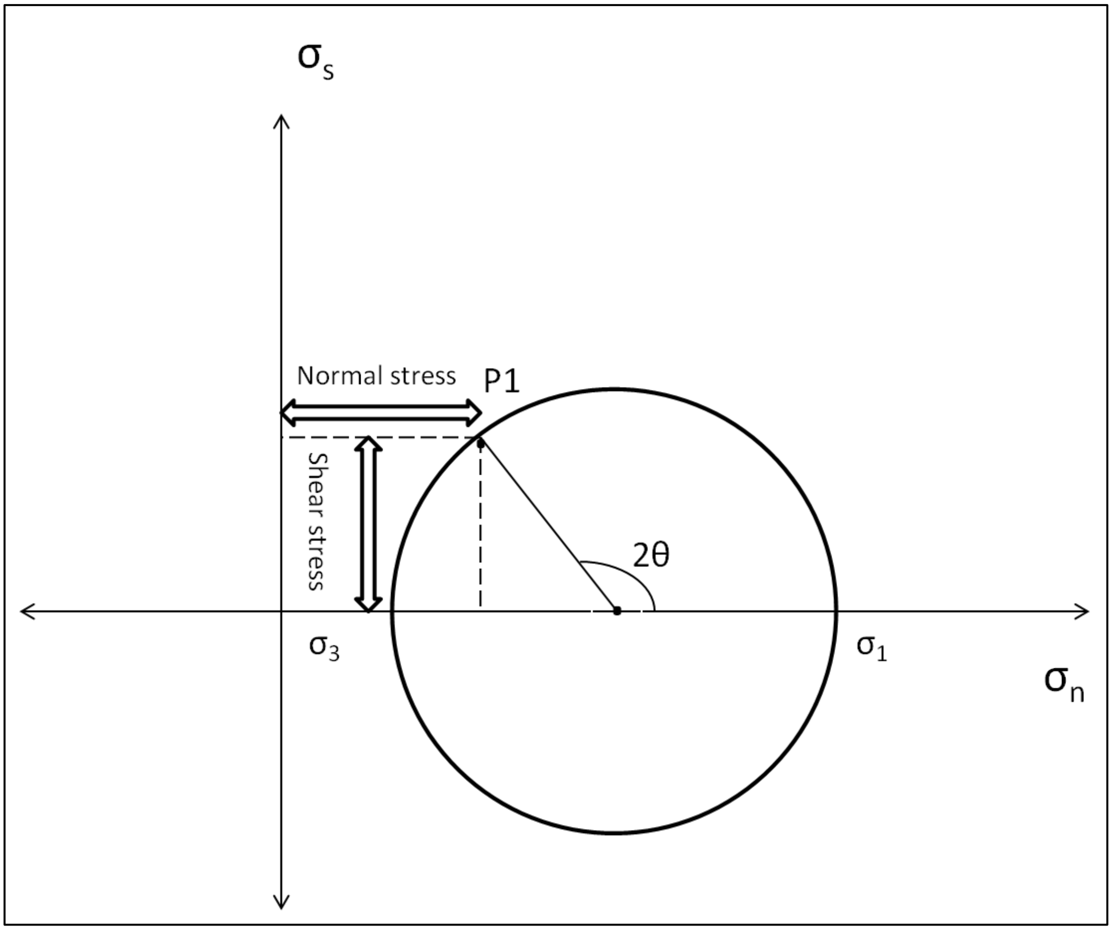

Figure 11 Mohr Circle showing components of Normal stress (σ_n) and shear stress (τ) in 2D

4.2.4. Mohr circle explained in three dimensions:

The previous discussion was mainly based on Mohr circle in 2D. When the three main stresses are displayed along the horizontal axis, the Mohr circle can also be used to depict the state of stress in three dimensions which is in fact a more realistic approach. To illustrate Mohr circle in three dimensions, three distinct circles are considered and are plotted parallel to the principal plane of stress (i.e. the plane containing σ_1- σ_2, σ_1- σ_3, σ_2- σ_3) (Fig 12). σ_2 is the intermediate principal stress axis and is plotted between

σ_1 and σ_3. Magnitudes of the three principal stress axes determine the radii of the circles.

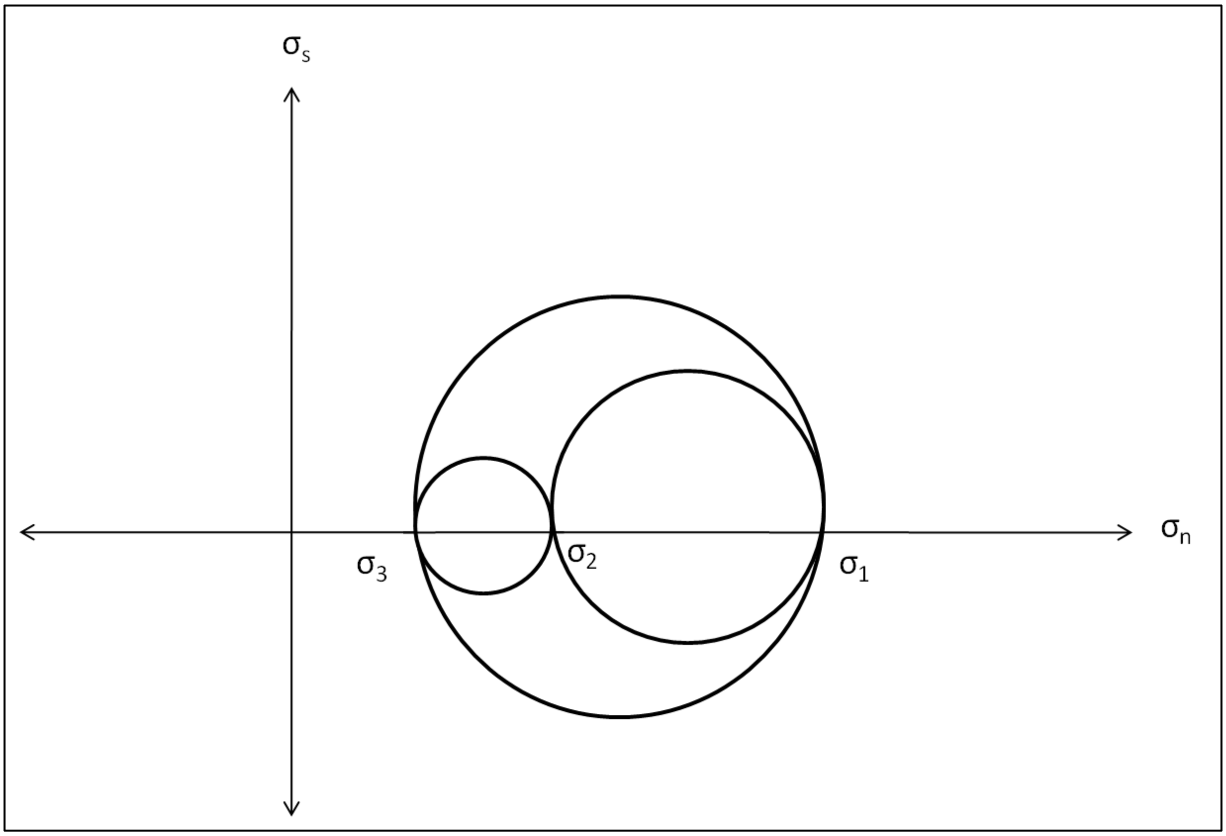

Figure 12 Mohr Circle in 3D

4.3. Plotting dyke orientations to find out stress direction and magnitude:

Older joints can be filled up by magma if magmatic pressure overcomes the horizontal stress acting across the joint plane. The pre-existing fabrics/fractures can only open when P_f surpasses normal stress (σ_n) (Delaney et al., 1986).

The condition, $P_f \geq \sigma_n$ (12)

Delaney et al., (1986) presented two equations to describe the opening of a fracture when $P_f > \sigma_n$. They are as follows:

$$\sigma_n = \frac{\sigma\max + \sigma\min}{2} + \frac{\sigma\max - \sigma\min}{2}\cos 2\theta \tag{13}$$

Substituting equation (13) in equation (12),

$$R = \frac{Pf - \frac{\sigma\max + \sigma\min}{2}}{\frac{\sigma\max - \sigma\min}{2}} = \frac{Pf - \sigma\mathrm{m}}{\tau max} \geq \cos 2\theta \tag{14}$$

R is the driving stress ratio, P_f is the fluid pressure, σ_{max} and σ_{min} are maximum and minimum principal stress respectively, σ_m is the mean stress, $\tau\mathrm{max}$ is the maximum shear stress and θ is the angle between the maximum principal stress and the normal to the fracture plane.

Later, the technique was expanded to three dimensions and two new equations were given by Baer et al., (1994) to represent the stress and P_f states.

$$R' = \frac{Pf - \sigma3}{\sigma1 - \sigma3} \tag{15}$$

$$\Phi = \frac{\sigma2 - \sigma3}{\sigma1 - \sigma3} \tag{16}$$

R' is the driving pressure ratio and It describes the relationship between the magnitude of the fluid pressure and maximum and minimum primary stresses (Baer et al., 1994).

Whereas, Φ is the stress ratio and it describes the relative magnitudes of the principal compressive stresses (Angelier, 1984; Baer et al., 1994).

R' by Baer et al. (1994) is not the same as the R ratio of Delaney et al. (1986) since it compares P_f with σ_3 instead of the mean stress (σ_m).

Fractures do not open when R' < 0, but can open in a variety of directions depending on the stress ratio (Φ) when R' > 0 (Baer et al., 1994).

The previuous theory was further modified by Jolly and Sanderson (1997) where they included the stereographic projections of the dyke orientaions to find out the paleostress orientation. Following the same procedure, in the first step 149 field measurements of mafic dykes from the study area (Ghatogaon and surroundings) are plotted in the stereonet software. In the next step their poles are also plotted. Depending on the density of the ploes a contour map of the same is also generated. According to Jolly and Sanderson (1997), if the dykes have similar orientations, a Clustered distribution of the poles to the dyke orientations is attained under the condition $P_f < \sigma_2$. Whereas in case of the dykes having different orientations, a Griddle distribution of poles to the dyke orientaions is attained under the condition $P_f > \sigma_2$. In our case the distribution is of Griddle type (Fig). Continuing with the procedure an empty space is identified and a best-fitting ellipse is drawn. The centre of the ellipse indicates the σ_1 direction (normal to the gridle distribution). Long and short axis of the ellipse is also drawn. σ_1-σ_2 and σ_1-σ_3 planes are recognised and the angles θ_3 and θ_2 are also determined on the planes respectively. For the griddle distribution ($P_f > \sigma_2$) the driving pressure ratio (R’) and the stress ratio (Φ) are calculated using equations 17 and 18 respectively.

$$R' = \frac{Pf - \sigma 3}{\sigma 1 - \sigma 3} = \frac{1 + cos2\theta 2}{2} \tag{17}$$

$$\Phi = \frac{\sigma 2 - \sigma 3}{\sigma 1 - \sigma 3} = 1 - \frac{1 - cos2\theta 2}{1 - cos2\theta 3} \tag{18}$$

5. Results and discussion (Petrography and Structural analysis):

In the current study 149 dyke orientations have been taken from the field area (Ghatagaon, Bhimkund and surroundings). From these dykes, sampling has been done where needed. Grain size variation within the dykes plays a major role to select outcrops for sampling. Detailed petrography has been done on the dyke samples to shed light on the local scale deformation and tectonics associated with these dykes and the surrounding country rock (Fig 13).

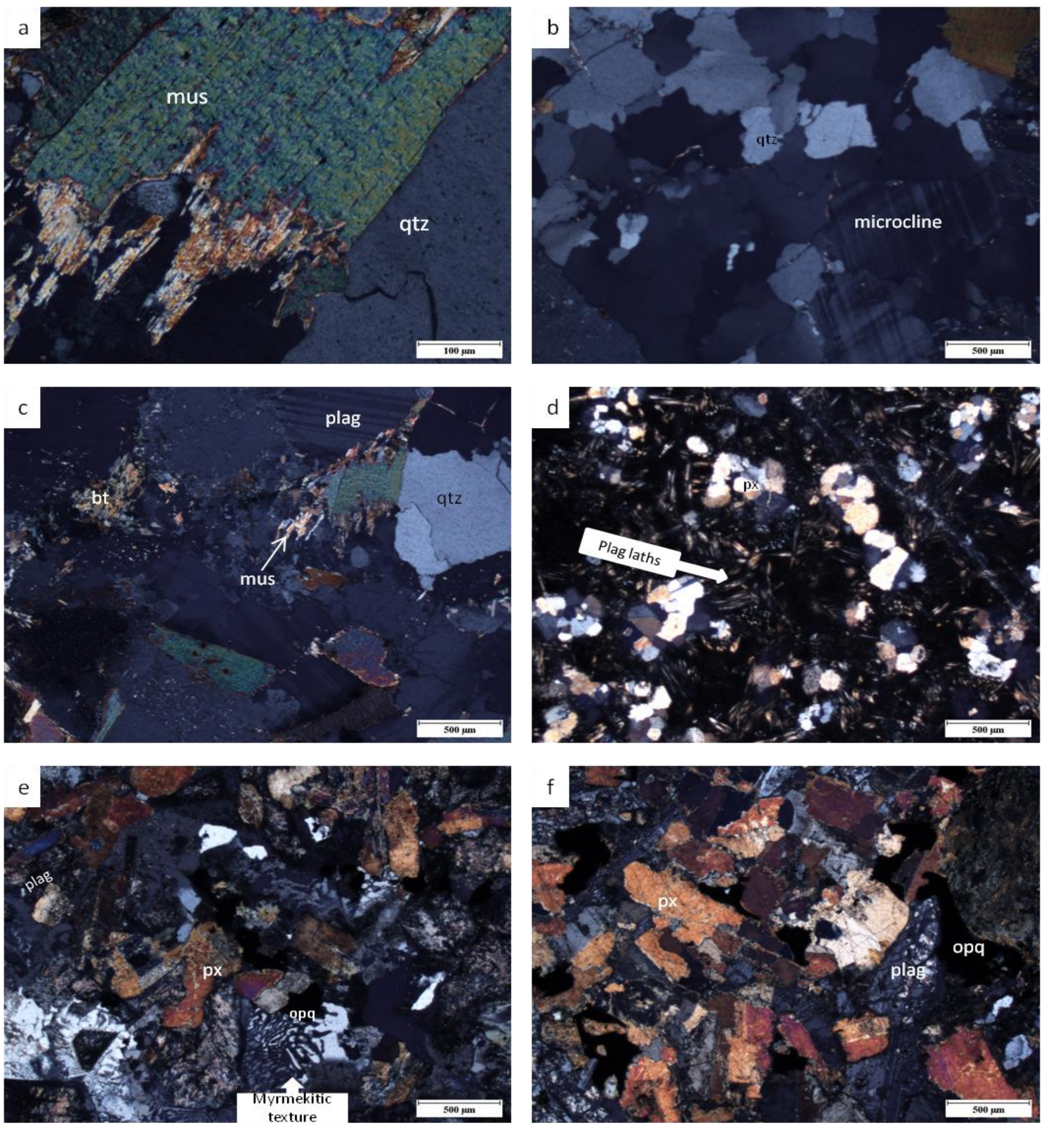

Figure 13

Fig 13 (a) XPL view of sample of granitic country rock. Muscovite and quartz are seen to be reacting to give rise to another mineral (most possibly Sillimanite), indicating high grade metamorphic event of Granulite facies. (b) Serrated grain boundary is seen among quartz grains under crossed polars. This indicates differential growth and also suggests that the minerals have suffered differential stress during their growth. The deformation leads to this serrated or jagged pattern of grain boundary. (c) XPL view of the country basement. (d) Thin section of fine-grained dyke sample from Bhimkund region under crossed polars showing ophitic texture between plagioclase laths and pyroxene grains. (e) Thin section of relatively coarser-grained dyke sample from Anandapur region under crossed polars with deformed plagioclase and pyroxene grains and showing myrmekitic texture between quartz and k-feldspar. (f) Coarser-grained dyke showing fractured plagioclase grains indicating local scale deformation that has affected the mineral grains during their growth.

Structural Analysis

From the 149 dyke orientations that have been taken, majorly two sets of dykes having trends of NW-SE and NE-SW are noticed. Stereographic plot of the dykes indicates that the number of dykes striking NW-SE is greater in number. The poles to the dykes are plotted in Stereonet software. According to Jolly and Sanderson (1997), the distribution of the poles show a 'Griddle' type of pattern that suggests numerous fractures were dilated (Fig 14C). In the next step the contour map of the same is also generated. That also supports the Griddle type of distribution. Continuing the method, an empty space is discovered in between the poles to the dykes and a best-fitting ellipse is drawn. Fractures were not dilated inside the ellipse, but those outside were dilated. Fractures around the center of the ellipse did not dilate, resulting in the σ_1 value. σ_1-σ_2 and σ_1-σ_3 planes are recognized and the angles θ_3 and θ_2 are also determined on the planes respectively. On the stereogram, θ angles are measured between the principal stress axes and the edge of the ellipse. θ_2 is measured on the σ_1-σ_3 plane and its value comes around 22 °. On the other hand, θ_3 is measured on the σ_1-σ_2 plane and its value comes around 62 °. Driving pressure ratio (R') is calculated from equation 17, which is 0.86. The stress ratio (Φ) is found to be 0.82 from equation 18. A 3D Mohr Circle is constructed with the orientations of σ_1, σ_2 and σ_3 from the stereoplot. From that calculations P_f value (Fluid Pressure) comes around 8.74 MPa (calculated from equation 15) that is definitely greater than the σ_2 value (Calculated from equation 16) which is found to be around 8.38 MPa. The P_f value is close to σ_1 ($\sigma_2 < P_f < \sigma_1$) and it automatically supports our distribution to be a Griddle type itself.

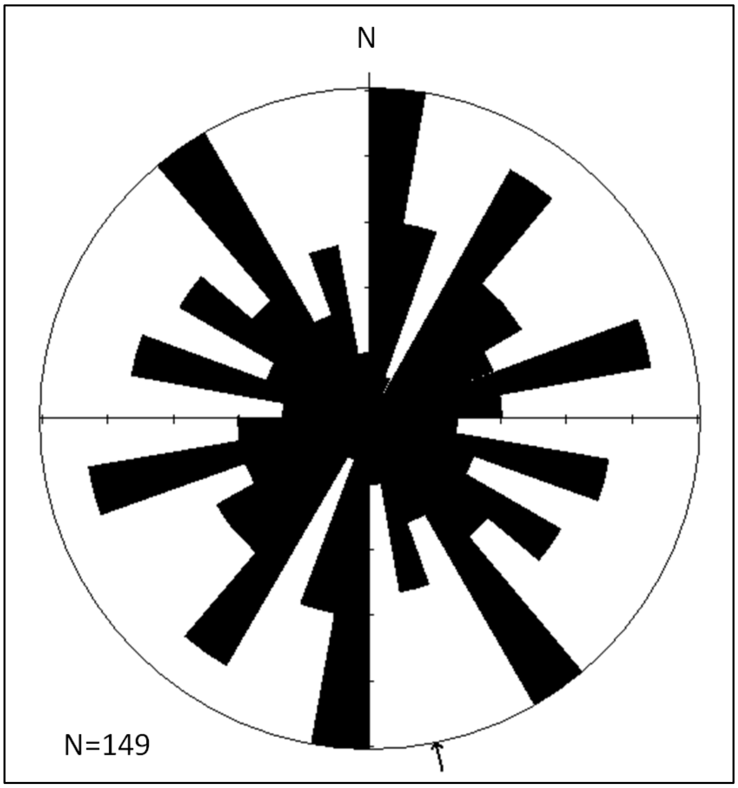

Figure 14 (a)

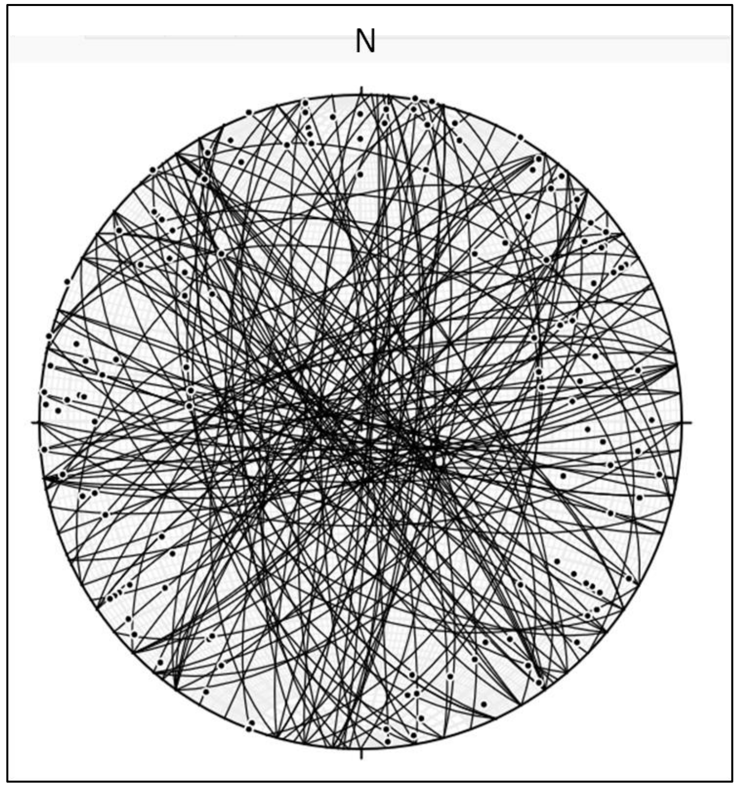

Figure 14 (b)

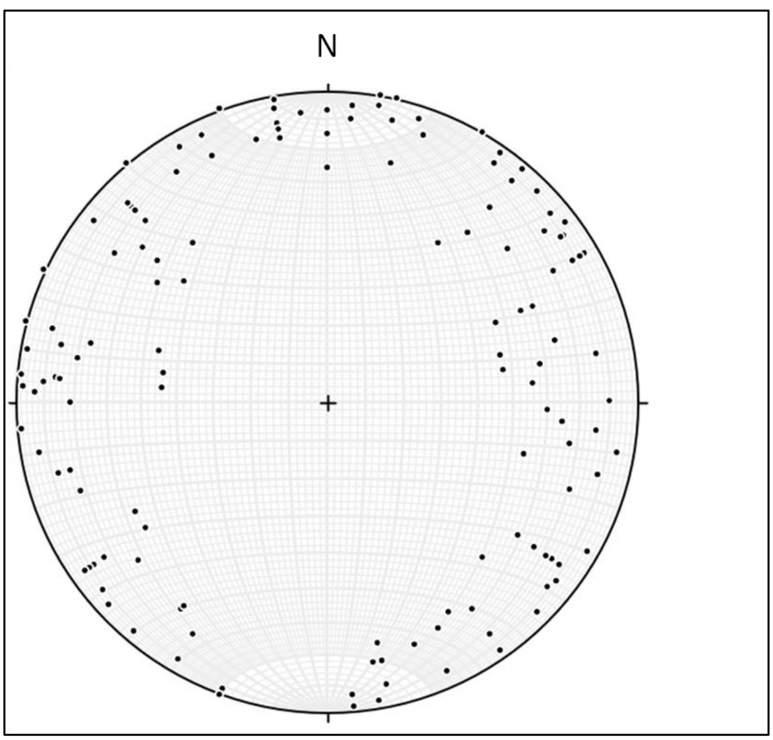

Figure 14 (c)

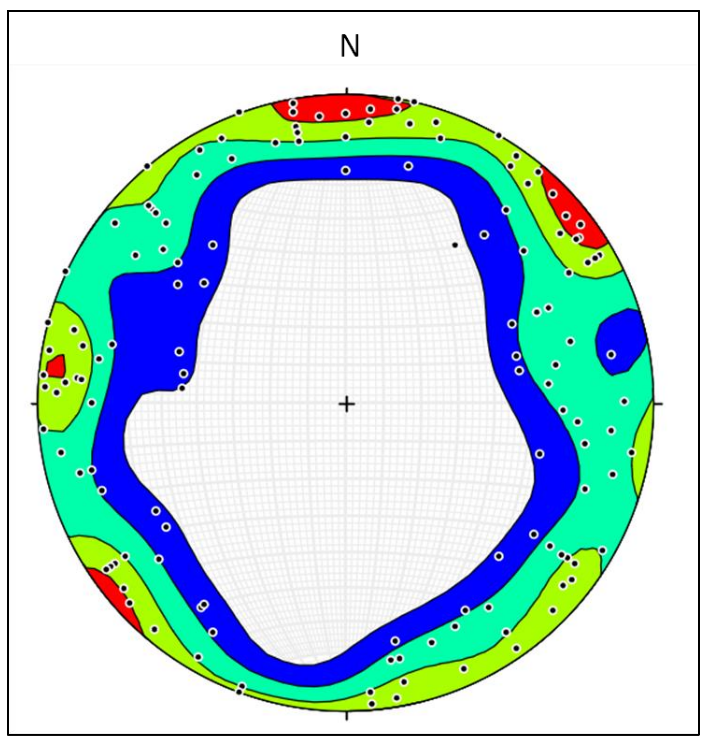

Figure 14 (d)

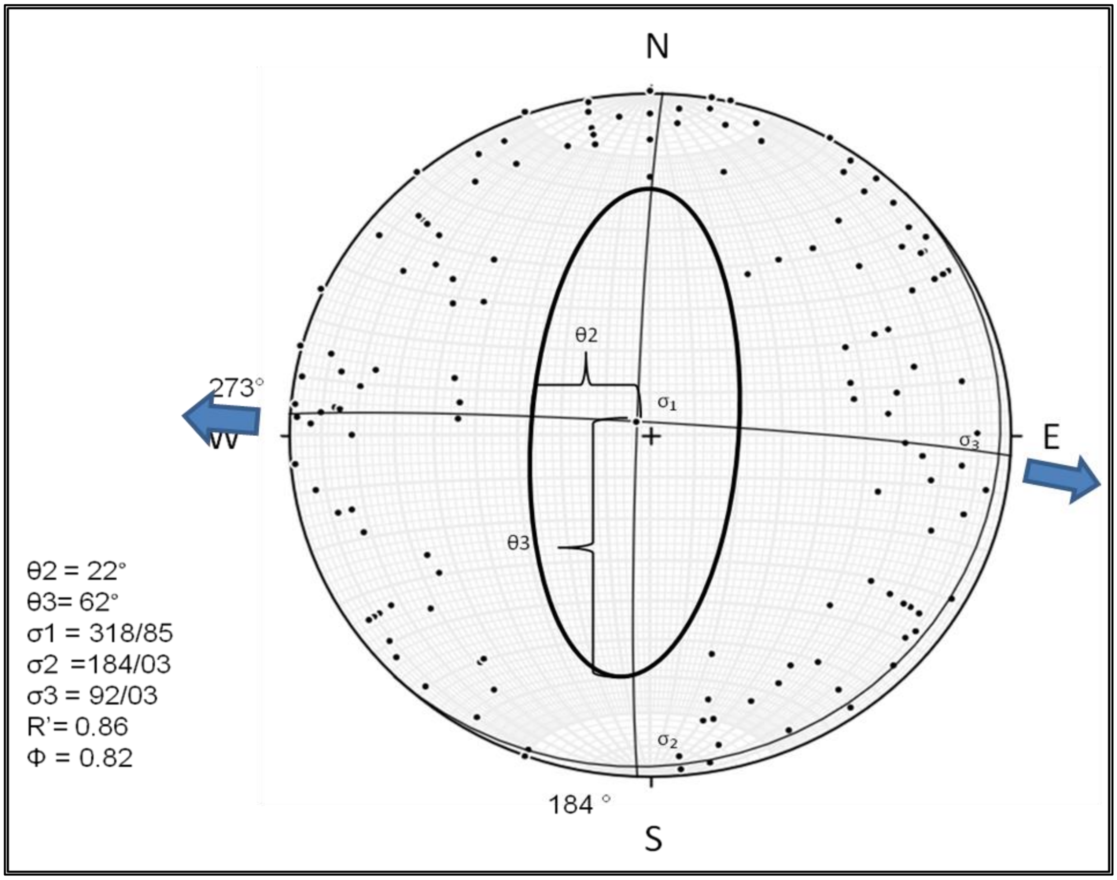

Figure 14 (e)

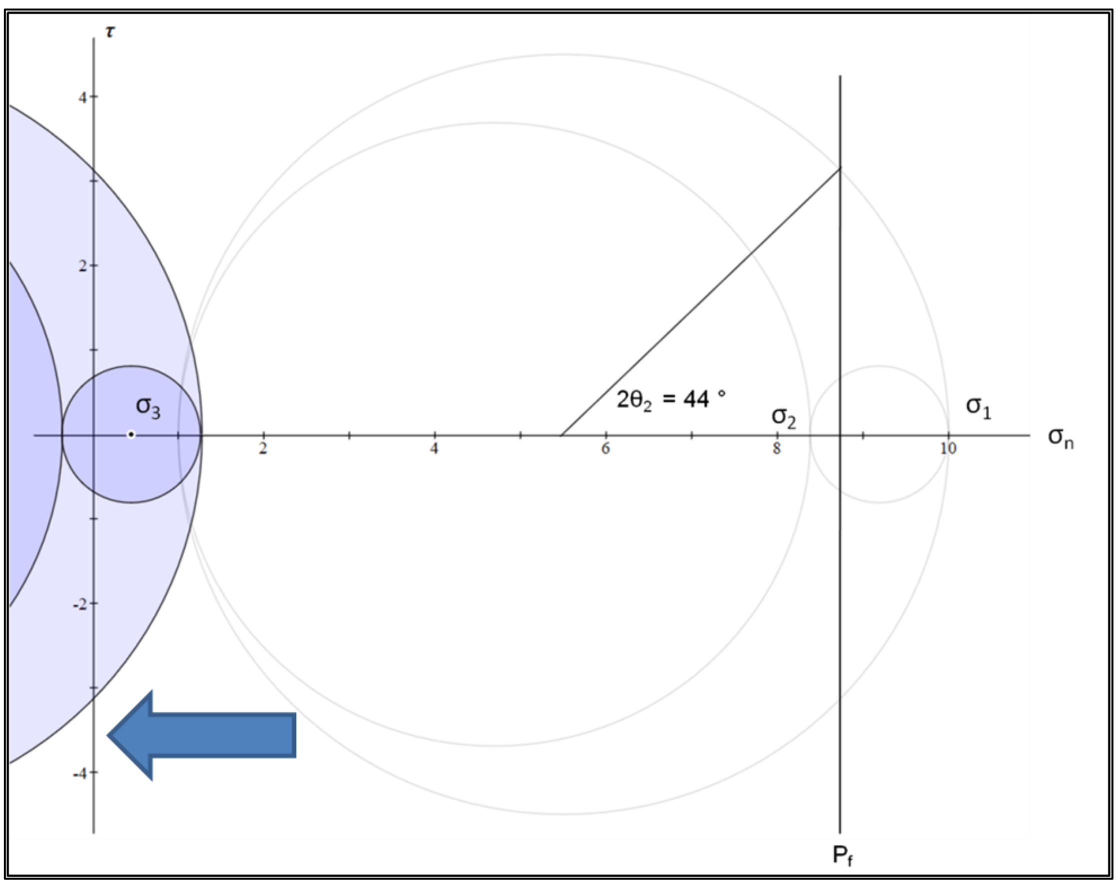

Figure 14 (f)

Fig 14 (a) : Rose diagram of dyke orientation data from the study area (Ghatagaon and surroundings). (b) Stereonet plot of the dyke orientations. (c) Poles to the dyke plotted in Stereonet software. (d) Contoured plot of the poles to the dykes that shows griddle distribution. (e) σ_1, σ_2 and σ_3 orientations are measured from the griddle distribution of the dyke orientations from the study area. θ_2 and θ_3 are also measured from the best-fitting ellipse that is drawn in between the free space of the stereonet plot of the poles to the dykes. (f) 3D Mohr Circle from dyke orientation data is constructed in MohrPlotter software. R' (Driving pressure ratio) and Φ (Stress ratio) are calculated 0.86 and 0.82 respectively. This is a relative stress illustration (not an absolute stress representation) based on the stress ratio (Φ). Fluid Pressure (P_f) value comes around 8.74 MPa. The boundary line of P_f is marked on the diagram upto where fracture can be dilated and dyke can be intruded. The left side of the P_f boundary line the magnitude of the normal stress is lesser than the P_f. Hence as per the generalized theroy of Jolly and Sanderson (1997) the fractures can be dilated in this region. The right side of the boundary line denotes greater mormal stress value than the P_f and thus there will not be any dilation. Fluid pressure acts opposite to the normal stress and it compels the Mohr Circle to shift leftwards.

6. Conclusion:

- The trend and plunge of the σ_1, σ_2, σ_3 are 318/85, 184/03 and 92/03 respectively. Hence the extension direction σ_3 was sub horizontal in EES-WWN. σ_1 was sub vertical towards NW-SE direction and the σ_2 was sub horizontal in the SSW-NNE direction.
- From the petrography of the host rock we can infer that the country granite has been highly metamorphosed and also the minerals have suffered differential stress during their growth that has created the jagged grain boundary.
- The high stress ratio ($\Phi = 0.82$) exhibits an oblate stress ellipsoid whereas high R' value refers to high P_f value that indicates opening of preexisting fractures in various directions which is also supported by the griddle type of distribution in stereoplot.
- The Mohr Circle plot refers to the stress setting to be an extensional type.
- This study refers to relative magnitudes of the principal stresses and not the absolute values. If we get the actual fluid inclusion data from the field, absolute magnitudes of the principal stresses can be obtained.

References

Baer, G., Beyth, M. and Reches, Z. (1994) Dikes emplaced into fractured basement, Timna Igneous Complex, Israel.- Journal of Geophysical Research 99.24039-2405 I.

Bandyopadhyay, P. K., Chakrabarti, A. K., DeoMurari, M. P., & Misra, S. (2001). 2.8 Ga old anorogenic granite-acid volcanics association from western margin of the Singhbhhum Orissa Craton. Gondwana Research, 4, 465–475.

Banerji, A. K. (1962). Cross folding, migmatization and ore localization along part of the Singhbhum Shear Zone, south of Tatanagar, Bihar, India. Economic Geology, 57, 50–71.

Banerji, A. K. (1969). A reinterpretation of the geological history of Singhbhum Shear Zone, Bihar. Journal of the Geological Society of India, 10, 49–55.

Banerji, A. K. (1977). On the Precambrian banded iron formation and manganese ores of the Singhbhum region, eastern India. Economic Geology, 72, 90–98.

Biswal, T. K., & Sinha, S. (2003). Deformation history of the NW salient of the Eastern Ghats Mobile Belt, India. Journal of Asian Earth Science, 22, 157–169.

Currie, K. L. and Ferguson, J. (1970) The mechanism of intrusion of lamprophyre dykes indicated by ‘offsetting’ of dikes. Tectonophysics 9, 525-535.

Currie, K. L. and Ferguson, J. (1970) The mechanism of intrusion of lamprophyre dikes indicated by ‘offsetting’ of dikes. Tectonophysics 9, 525-535.

Dasgupta, P., Ray, A. & Chakraborti, T.M. Geochemical characterisation of the Neoarchaean newer dolerite dykes of the Bahalda region, Singhbhum craton, Odisha, India: Implication for petrogenesis. J Earth Syst Sci 128, 216 (2019). https://doi.org/10.1007/s12040-019-1228-0.

Delaney, P. T., Pollard, D. D., Zioney, J. 1. and McKee, E. H. (1986) Field relations between dikes and joints: Emplacement processes and paleostress analysis. Journal of Geophysical Research 91,492&4938.

Ghosh, D. K., Sarkar, S. N., Saha, A. K., & Ray, S. L. (1996). New insights on the early Archaean crustal evolution in eastern India: Re-evaluation of lead-lead, samarium-neodymium and rubidium-strontium geochronology. Indian Minerals, 50, 175–188.

Iyengar, S. V. P., & Murthy, Y. G. K. (1982). The evolution of the Archaean-Proterozoic crust in parts of Bihar and Orissa, eastern India. Record Geological Survey of India, 112, 1–5.

Jolly, R.J.H., Sanderson, D.J., 1995. Variation in the form and distribution of dykes in the Mull swarm, Scotland. J. Struct. Geol. 17, 1543–1557.

Jolly, R.J.H., Sanderson, D.J., 1997. A Mohr circle reconstruction for the opening of a preexisting fracture. J. Struct. Geol. 19, 887–892.

Mahalik, N. K. (1994). Geology of the contact between the Eastern Ghats belt and North Orissa Craton. Journal of the Geological Society of India, 44, 41–51.

Manu Prasanth MP, Pang K-N, Hari KR, Sahoo BB, Ravindran A and Iizuka Y (2023) Geochemistry of Precambrian dyke swarms in the Singhbhum craton, India: Implications for recycled crustal components in the mantle source. Front. Earth Sci. 10:1092823. doi: 10.3389/feart.2022.1092823.

Martinez-Poza, A.I., Druguet, E., 2016. Structure and tectonic setting of the SE Sardinia mafic dyke swarm. Insights for the stress state during magma emplacement in the upper crust. J. Geodyn. 101, 170–185.

Mazzarini, F., Musumeci, G., Cruden, A.R., 2011. Vein development during folding in the upper brittle crust: the case of tourmaline-rich veins of eastern Elba Island, northern Tyrrhenian Sea, Italy. J. Struct. Geol. 33, 1509–1522.

Mazzarini, F., Musumeci, G., 2008. Hydrofracturing-related sill and dyke emplacement at shallow crustal levels: the Eastern Elba Dyke Complex, Italy. Geol. Soc. Lond. Spec.Publ. 302 (1), 121–129.

Mondal, T.K., Mamtani, M.A., 2013. 3-D Mohr circle construction using vein orientation data from Gadag (southern India)–implications to recognize fluid pressure fluctua tion. J. Struct. Geol. 56, 45–56.

Mukhopadhyay, D., 2001, The Archaean nucleus of Singhbhum: the present state of knowledge. Gondwana Research, v. 4, pp. 307-318.

Mukhopadhyay, Dhruba, and Abdul Matin. "The architecture and evolution of the Singhbhum Craton." Episodes Journal of International Geoscience 43.1 (2020): 19-50.

Mukhopadhyay, D. (1976). Precambrian stratigraphy of Singhbhum: The problem and a prospect. Indian Journal of the Earth Sciences, 3, 208–219.

Murty, V. N., & Acharya, S. (1975). Lithostratigrtaphy of the Precambrian rocks around Koira, Sundargarh district, Orissa. Journal of the Geological Society of India, 16, 55–68.

Pandey, Om Prakash, Klaus Mezger, Dewashish Upadhyay, Debajyoti Paul, Ajay Kumar Singh, Ulf Söderlund, and Ashley Gumsley. "Major-trace element and Sr-Nd isotope compositions of mafic dykes of the Singhbhum Craton: Insights into evolution of the lithospheric mantle." Lithos 382 (2021): 105959.

R. Mir, Akhtar. 2022. ‘Proterozoic Newer Dolerite Dyke Swarm Magmatism in the Singhbhum Craton, Eastern India’. Geochemistry and Mineral Resources. IntechOpen. doi:10.5772/intechopen.104833.

Ray, Arijit. (2012). Newer Dolerite dykes, Jharkhand, India: A case study of magma generation, differentiation and metasomatism in a subduction zone setting. GEOCHEMICAL JOURNAL. 46. 10.2343/geochemj.1.0174.

Roberts, J. L. and Sanderson, D. J. (1971) The intrusive form of some basaltic dykes showing flow lineation. Geological Magazine 108,489- 499.

Saha, A., Basu, A. R., Garzione, C. N., Bandyopadhyay, P. K., & Chakrabarti, A. (2004). Geochemical and petrological evidence for subduction—Accretion processes in the Archaean Eastern Indian Craton. Earth and Planetary Science Letters, 220, 91–106.

Saha, A. K., Ray, S. L., Ghosh, S., Mukhopadhyay, K., & Dasgupta, P. (1984). Studies in crustal evolution of the Singhbhum-Orissa Iron Ore Craton. Crustal Evolution of Parts of Indian Shield (pp. 1–74). Kolkata: Indian Society of Earth Scientists.

Saha, A. K. (1994). Crustal evolution of Singhbhum, North Orissa, Eastern India. India, Bangalore: Geological Society. 341 p.

Saha, A. K., Ray, S. L., & Sarkar, S. N. (1988). Early history of the Earth: Evidence from the eastern Indian shield. In D. Mukhopadhyay (Ed.), Precambrian of the Eastern Indian Shield (pp. 13–37). India, Bangalore: The Geological Society.

Sarkar, S. C. (2000). Crustal evolution and metallogeny in the Eastern Indian Craton. Special Publication of the Geological Survey of India, 55, 169–194.

Sarkar, S.C. and Gupta, A., 2012, Crustal evolution and metallogeny in India. Cambridge University Press. pp. 840.

Sarkar, S. N., & Saha, A. K. (1962). A revision of the Precambrian stratigraphy and tectonics of Singhbhum and adjacent region. Quaternary Journal of Geology Mining Metallurgy Society of India, 34, 97–136.

Sarkar, S. N., & Saha, A. K. (1983). Structure and tectonics of the Singhbhum-Orissa iron ore craton, Eastern India. In S. SinhaRoy (Ed.), Structure and tectonics of Precambrian rocks of India (pp. 1–25). Delhi: Hindustan Publishing Corporation.

Sengupta, S., Paul, D. K., de Laeter, J. R., McNaughton, N. J., Bandyopadhyay, P. K., & Smith, J. B. (1991). Mid-Archaean evolution of the eastern Indian craton: Geochemical and isotopic evidence from the Bonai pluton. Precambrian Research, 49, 23–37.

Shankar, Ravi, B. Vijayagopal, and Anil Kumar. "Precise Pb-Pb Baddeleyite Ages of 1765 Ma for a Singhbhum'Newer Dolerite'Dyke Swarm." Current Science (2014): 1306-1310.

Sharma, M., Basu, A. R., & Ray, S. L. (1994). Sm-Nd isotopic and geochemical study of the Archaean tonalite-amphibolite association from eastern Indian craton. Contributions to Mineralogy and Petrology, 117, 45–55.

Annexure

Table 1 149 dyke measurements (dip amount and dip directions) from the study area.

Dyke No	Dip amount	Dip direction
1	71	165
2	71	90
3	70	100
4	60	315
5	82	193
6	32	12
7	40	15
8	48	15
9	25	45
10	45	30
11	58	245
12	44	100
13	60	60
14	44	95
15	35	330
16	45	210
17	50	245
18	80	200
19	90	190
20	52	215
21	68	50
22	85	198
23	62	245
24	68	195
25	85	233
26	90	160
27	82	220
28	70	220
29	85	240
30	85	225
31	78	232
32	73	240
33	65	230
34	60	220
35	73	70
36	85	47
37	86	40

38	88	20
39	90	20
40	75	30
41	70	35
42	90	210
43	69	35
44	88	355
45	85	30
46	80	325
47	82	193
48	90	193
49	86	190
50	65	255
51	84	355
52	47	107
53	90	105
54	68	280
55	50	130
56	83	55
57	76	95
58	76	102
59	90	115
60	88	95
61	80	105
62	86	300
63	84	280
64	76	276
65	77	305
66	83	92
67	80	105
68	75	95
69	84	128
70	80	94
71	66	130
72	67	104
73	56	345
74	56	140
75	82	348
76	68	348
77	74	348
78	56	125
79	72	290
80	70	334
81	80	305
82	64	305

83	70	305
84	79	285
85	75	305
86	70	325
87	60	130
88	84	155
89	80	325
90	85	170
91	80	170
92	87	350
93	88	170
94	80	270
95	55	285
96	77	260
97	65	275
98	90	140
99	85	315
100	87	325
101	82	310
102	80	185
103	78	170
104	74	350
105	72	340
106	74	75
107	78	75
108	80	55
109	82	55
110	83	50
111	84	55
112	58	245
113	80	240
114	48	255
115	48	260
116	59	260
117	56	265
118	83	240
119	82	235
120	81	235
121	64	180
122	75	180
123	75	170
124	76	165
125	60	55
126	76	55
127	83	215

128	87	215
129	87	220
130	83	230
131	87	100
132	87	93
133	78	135
134	83	80
135	67	330
136	84	336
137	84	150
138	79	135
139	83	308
140	85	185
141	77	147
142	60	272
143	71	135
144	76	135
145	76	155
146	83	180
147	82	175
148	72	125
149	88	85